



## CPT-based evaluation of liquefaction-induced settlement for reclaimed gravelly soil

Riwaj Dhakal<sup>1</sup> and Misko Cubrinovski<sup>2</sup>

<sup>1</sup>Postdoctoral Research Fellow, Department of Civil and Natural Resources Engineering, University of Canterbury, Christchurch, New Zealand

<sup>2</sup>Professor, Department of Civil and Natural Resources Engineering, University of Canterbury, Christchurch, New Zealand  
[\\*riwaj.dhakal@canterbury.ac.nz](mailto:riwaj.dhakal@canterbury.ac.nz) (Corresponding Author)

### ABSTRACT

Gravelly soils are not well represented in current semi-empirical liquefaction evaluation procedures, which raises the question whether state-of-the-practice liquefaction evaluation methods, which are predominantly based on clean sands and sands with fines, are applicable to gravelly soils. In particular, the Cone Penetration Test (CPT) liquefaction settlement evaluation procedure uses empirical correlations between relative density ( $D_R$ ) and penetration resistance based on laboratory tests of clean sand. These procedures therefore do not account for the effects of particle size on penetration resistance through the effects of the packing of the soil. This paper investigates the applicability of a CPT –  $D_R$  correlation developed for a wide range of liquefiable soils including gravels in the liquefaction-induced settlement evaluation for well-graded reclaimed gravelly soil. The correlation is first shown to capture the effects of grain size composition on the penetration resistance through the index void ratios  $e_{max}$  and  $e_{min}$ . A developing novel methodology for evaluation of  $e_{max}$  and  $e_{min}$  for gravel-sand-silt mixtures including results from preliminary laboratory tests are then presented. Finally, results of liquefaction-induced settlement estimates based on the employed CPT –  $D_R$  correlation are compared with results obtained using sand-based empirical correlations for the well-documented liquefaction case history of CentrePort (New Zealand). Results show that sand-based procedures for evaluation of liquefaction-induced settlement are found to overestimate the relative density and consequently underestimate post-liquefaction settlement of gravelly soils as compared to using correlations accounting for grain-size effects on penetration resistance, particularly at medium to high densities. However, these differences are smaller for well-graded gravels that have a dominant silty sand fraction in the soil matrix deposited in a loose state.

Keywords: gravelly soil, cone penetration test, post-liquefaction settlement, relative density, index void ratios.

### INTRODUCTION

Reclaimed land is typically constructed using available soils from nearby sources, and there are number of case histories in which constructed fills comprise gravel-sand-silt (G-S-S) mixtures. Such reclamations often host important facilities and critical infrastructure, and hence their performance during earthquakes is of great significance [1]. One of the principal objectives in the liquefaction assessment is to quantify the liquefaction-induced damage to land and structures including loss of bearing capacity, transient ground deformations, and permanent ground displacements. In simplified procedures, free-field ground settlement is evaluated using methods developed primarily using evidence from liquefaction case histories and laboratory tests on clean sands and sand with fines. The evaluation procedure involves the use of a field parameter (e.g., cone tip resistance in the Zhang et al. [2] settlement evaluation) to estimate the relative density ( $D_R$ ) of the sand, for subsequent estimation of liquefaction-induced volumetric strains and settlement. While estimating  $D_R$  from in-situ tests through empirical correlations for clean sands and sands with small amount of silt (e.g., < 15%) is relatively straightforward, albeit involving significant uncertainties, more serious issues are encountered when performing such conversions for gravelly soils [3; 4], since gravelly soils affect all aspects of the behavior differently from clean sands. For example, the presence of larger gravel-size particles and lower volume of voids in gravels significantly affects (increases) penetration resistance [5]. Hence, many existing correlations derived based on clean sands do not account for these effects of gravelly soils on penetration resistance. Additional issues are encountered in the implementation of  $D_R$  concepts for gravelly soils as determination of index void ratios ( $e_{max}$  and  $e_{min}$ ), which are required for evaluation of  $D_R$ , have not been firmly established yet for gravelly soils.

This paper examines the use of several CPT-based  $D_R$  correlations derived for clean sands with one correlation developed for a wide range of soils including sandy and gravelly soils in the evaluation of liquefaction-induced settlement for representative CPT profiles from the well-documented case history of the port of Wellington, New Zealand (CentrePort). The paper scrutinizes issues related to the density state characterization of G-S-S reclamations in simplified CPT-based procedures which is subsequently used as a key parameter in the evaluation of liquefaction-induced settlement.

**ESTIMATING SETTLEMENT OF CLEAN SANDS**

Liquefaction-induced settlement is commonly estimated based on the procedure developed by Ishihara & Yoshimine [6] correlating factor of safety against liquefaction triggering ( $FS_L$ ) and the initial  $D_R$  of the soil to estimate post-liquefaction volumetric strain ( $\epsilon_v$ ). The empirical correlations of Ishihara & Yoshimine [6] were developed using laboratory test results on a single clean sand (Fuji River Sand; [7]). The relationships, using mathematical approximations by Yoshimine et al. [8], are shown in Figures 1a and 1b. Figure 1b shows that post-liquefaction volumetric strains vary strongly with the relative density of sand from approximately 1.2% (for very dense sand with  $D_R = 90\%$ ) to 4.4% (for loose sand with  $D_R = 40\%$ ). The results summarized in Figures 1a and 1b were then used to develop the chart for estimation of post-liquefaction volumetric strains shown in Figure 1c.

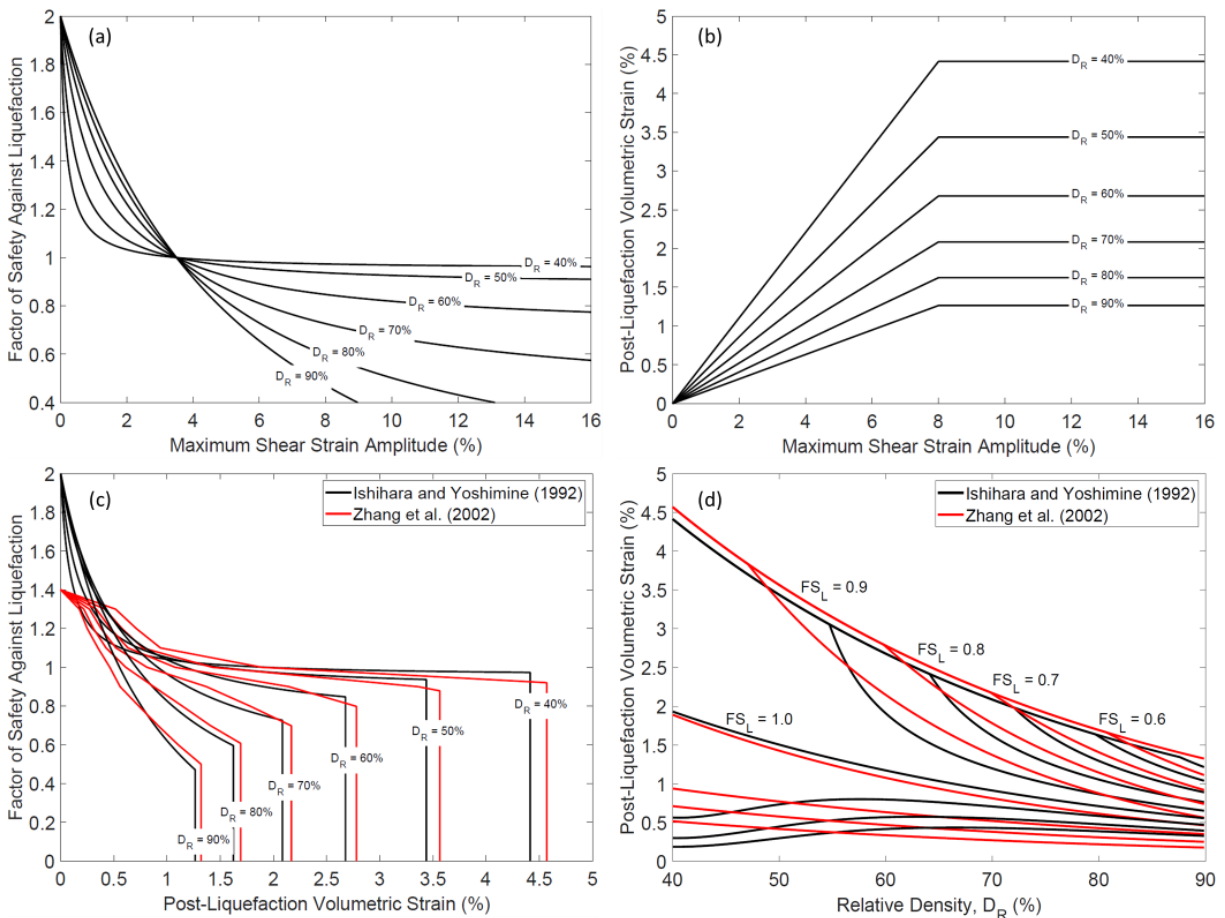


Figure 1. Ishihara & Yoshimine [6] relationships (shown in black) for clean sands using approximations by Yoshimine et al. [8] between (a)  $FS_L$  and maximum shear strain amplitude ( $\gamma_{max}$ ), and (b)  $\gamma_{max}$  and volumetric strain ( $\epsilon_v$ ), for given  $D_R$ . The resulting  $FS_L - \epsilon_v$  relationships for given  $D_R$  values are shown in (c) and (d) (equivalent Zhang et al. [2] curves are shown in red).

A key requirement in the application of these laboratory-based relationships to sand deposits in the field is to estimate the relative density of the sand using a field-based parameter (i.e., the cone tip resistance in the case of CPT-based assessment). This conversion involves significant uncertainties, as illustrated in Figure 2a showing correlations of  $D_R$  with clean-sand equivalent cone tip resistance ( $q_{cINcs}$ ), for clean sands developed by Tatsuoka et al. [9], Robertson & Cabal [10], and Idriss & Boulanger [11].

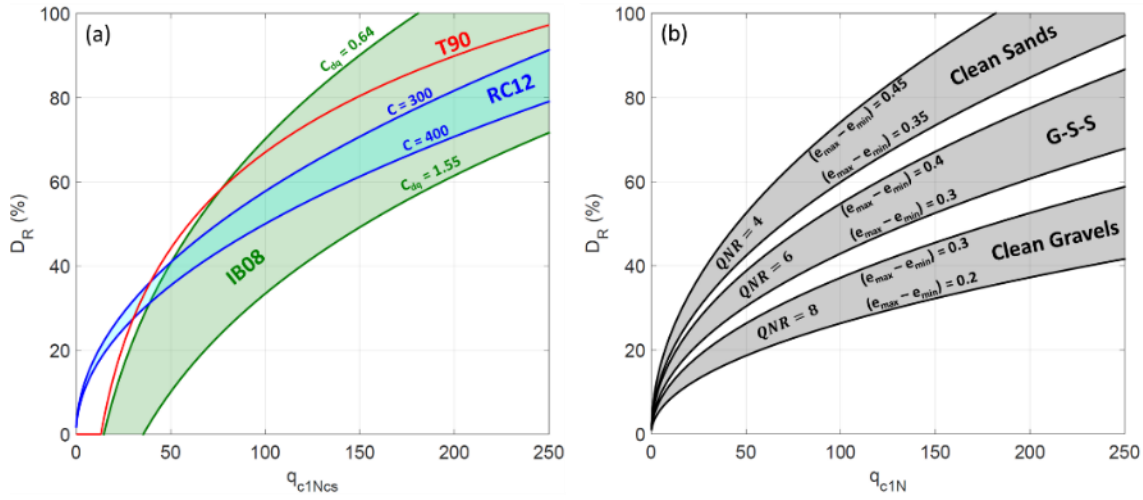


Figure 2. (a)  $D_R - q_{c1Ncs}$  correlations developed using sands by Tatsuoka et al. [9], denoted as T90, Robertson & Cabal [10], denoted as RC12, and Idriss & Boulanger [11], denoted as IB08, and (b) the Cubrinovski & Ishihara [5] SPT correlation with SPT-to-CPT conversion  $QNR$  values as noted for soils of varying grain-size distributions.

These three expressions, herein denoted T90, RC12 and IB08 are shown in Eq. (1)–(3), respectively.

$$D_R = -0.85 + 0.76 \log_{10}(q_{c1N}) \quad (1)$$

$$D_R = \sqrt{\frac{q_{c1N}}{c}} \quad (2)$$

$$D_R = 0.465 \left( \frac{q_{c1N}}{C_{dq}} \right)^{0.264} - 1.063 \quad (3)$$

For these equations,  $c$  is a material factor ranging between 300 and 400 for fine to coarse sands in the RC12 correlation, and  $C_{dq}$  is a material factor with characteristic values between 0.64 and 1.55 for the sands used in the development of the IB08 correlation, with an estimated mid-range value of  $C_{dq} = 0.9$ . It is apparent in Figure 2a that for a given  $q_{c1Ncs}$  of clean sand, there is a wide range of corresponding  $D_R$  values resulting from the empirical relationships.

Using the results from Ishihara & Yoshimine [6] as the basis, Zhang et al. [2] proposed CPT-based charts and mathematical expressions where  $D_R$  was converted to an equivalent  $q_{c1Ncs}$  for clean sand using the T90  $D_R - q_{c1Ncs}$  relationship. Figure 1d shows the conventional Zhang et al. [2] curves by converting their original  $q_{c1Ncs}$  chart back to  $D_R$  using T90. The relationships proposed by Ishihara & Yoshimine [6] and Zhang et al. [2] comparatively shown in Figure 1c and Figure 1d illustrates their equivalence.

Though the uncertainty in applying the  $\varepsilon_v - D_R$  relationships (Figure 1c and 1d) to clean sands has been highlighted, its application to other soils, such as G-S-S mixtures, is even more challenging due to two main reasons. Firstly, there is no direct evidence that the  $\varepsilon_v - D_R$  relationships derived for clean sand are appropriate for G-S-S mixtures. Secondly, even if the  $\varepsilon_v - D_R$  relationships are applicable to G-S-S mixtures, the conversion of  $q_{c1Ncs}$  to  $D_R$  for G-S-S mixtures requires some additional considerations. The latter issue is explored in greater depth in this paper.

## ISSUES IN THE APPLICATION OF SAND-BASED SETTLEMENT PROCEDURES TO G-S-S MIXTURES

While it is recognised that volumetric strain ( $\varepsilon_v$ ) – maximum shear strain amplitude ( $\gamma_{max}$ ) relationships from laboratory tests may be different for gravelly soil as compared to clean sand, this study focuses on another the application of the relationships of Figure 1 with respect to issues on estimating relative density via penetration resistance. The CPT penetration resistance in gravels is expected to be higher than sands, for all other conditions being equal, due to two important differences in the particle and packing characteristics of sands and gravels. Firstly, gravel particles are large relative to the penetration probe (cone size), which is known to lead to an increase in the penetration resistance, and in some cases may even result in refusal. The increase in the penetration resistance is particularly pronounced for clean medium-to-coarse gravels that have particle sizes comparable to the size of a conventional 10 cm<sup>2</sup> cone, even when the gravel is not very dense [12]. It is important to note that the G-S-S reclamations at CentrePort considered in this paper contain a high proportion of fine-to-medium sized weathered angular gravel, with 70–95% of the particles being less than 19 mm in size [13; 14]. In addition, testing at CentrePort was largely done using

a larger 15 cm<sup>2</sup> cone [15], which is considered standard practice. Thus, the combination of the smaller-sized angular gravel particles, sufficient content of finer sand and silt fractions, and larger penetration probe contributed to a generally successful performance of the CPT in the CentrePort gravelly fill largely overcoming issues related to the use of conventional CPTs in gravelly soils.

The second factor that leads to an increase of the penetration resistance in gravels is related to the denser packing or lower void ratios of gravels. Clean gravels have generally less voids in their structure, even when deposited in a loose state, as compared to sands and silts [16; 17]. Hence, gravels typically exhibit higher stiffness and strength, and consequently larger penetration resistance than sands. The important effects of larger particle size and lower volume voids on the penetration resistance in gravels, as well as different packing characteristics of gravelly soils, should be accounted for in the conversion from penetration resistance to  $D_R$  required for the estimate of settlement.

There are limited studies on the effects of grain-size on penetration resistance and its relationships with  $D_R$ . One such study is that of Cubrinovski & Ishihara [5] and Cubrinovski & Ishihara [18], which are important contributions investigating these effects. To the authors' knowledge, the empirical correlation between the normalized SPT blow count,  $(N_1)_{60}$ , and  $D_R$  proposed by Cubrinovski & Ishihara [5], herein denoted CI99 and shown in Eq. (4), is the only available correlation between the penetration resistance and  $D_R$  based on high-quality data for a wide range of soils including gravels, gravelly soils, sands, silty sands, and their mixtures.

$$(N_1)_{60} = D_R^2 \frac{11.7}{(e_{max} - e_{min})^{1.7}} \quad (4)$$

An important feature of the CI99 relationship is that it uses the void ratio range ( $e_{max} - e_{min}$ ) as an inherent material parameter that reflects the effects of overall grain-size composition and particle characteristics of cohesionless soil, and hence it embodies the combined influence of the entire grain composition and particle shapes of a given soil. Since the void ratio range is the difference between the two index void ratios ( $e_{max}$  and  $e_{min}$ ), it is a proxy for the deformation potential of the soil. Note that ( $e_{max} - e_{min}$ ) also features in the definition of  $D_R$ , shown in Eq. (5).

$$D_R = 100\% \times \frac{e_{max} - e}{e_{max} - e_{min}} \quad (5)$$

The ( $e_{max} - e_{min}$ ) values can therefore be used to represent the effects of grain-size on the  $D_R - (N_1)_{60}$  relationship of CI99 and hence use it to scrutinize the effects of fines and gravels on penetration resistance. Figure 3b illustrates an empirical relationship between ( $e_{max} - e_{min}$ ) and the median particle size of soils ( $D_{50}$ ), in which a clear trend for a reduction in ( $e_{max} - e_{min}$ ) is evident as the soil particle size increases. Additionally, Figure 3c illustrates an empirical relationship between ( $e_{max} - e_{min}$ ) and  $FC$  of sands with  $GC < 15\%$  and varying proportion of fines, in which a clear trend for an increase in ( $e_{max} - e_{min}$ ) is evident as  $FC$  increases. Apparently, the gravel-sized particles and finer silt-sized particles in the reclaimed G-S-S fills have opposing effects on ( $e_{max} - e_{min}$ ) and therefore on penetration resistance, as compared to sands. The former decreases ( $e_{max} - e_{min}$ ), leading to greater penetration resistances, while the latter increases ( $e_{max} - e_{min}$ ), leading to lower penetration resistances. Hence, while the voids in G-S-S mixtures are likely not as large as clean sands or sands with fines, they are expected to be larger than that of clean gravels, which is further supported by other studies such as Lin et al. [19] and Hara et al. [20].

A drawback of the CI99 correlation is that it was developed using SPT rather than CPT data. Thus, when applying it to CPT data, a conversion from  $(N_1)_{60}$  to  $q_{c1N}$  is required which adds an additional component of uncertainty. This conversion is done via  $QNR (= q_{c1N} / (N_1)_{60})$ , which can be estimated for different soil types based on empirical evidence [21]. The CI99 SPT-based correlation in Eq. (4) can therefore be expressed in terms of cone tip resistance in Eq. (6).

$$q_{c1N} = QNR \frac{11.7}{(e_{max} - e_{min})^{1.7}} D_R^2 \quad (6)$$

To illustrate the effects of soil characteristics on the  $D_R - q_{c1N}$  relationship of Eq. (6), Figure 2b plots the relationship using  $QNR$  and ( $e_{max} - e_{min}$ ) values typical for clean sands and clean gravels. Note that the CI99 relationship corresponding to clean sands is in general agreement with the sand-based relationships of T90, RC12 and IB08 in Figure 2a. Importantly, the relationships in Figure 2b depict the effects of particle size and grain-size composition of soils on the penetration resistance and indicate, for example, that at a given relative density, clean gravels exhibit larger penetration resistance than clean sands. This suggests that while penetration resistances are low for loose gravels, the conventional CPT resistance substantially increases for medium-to-dense gravels, and dense gravels are virtually impenetrable with a conventional CPT. In order to use Eq. (6) for G-S-S mixtures, accurately estimates of index void ratios are required to calculate void ratio range ( $e_{max} - e_{min}$ ), which is addressed in the subsequent section.

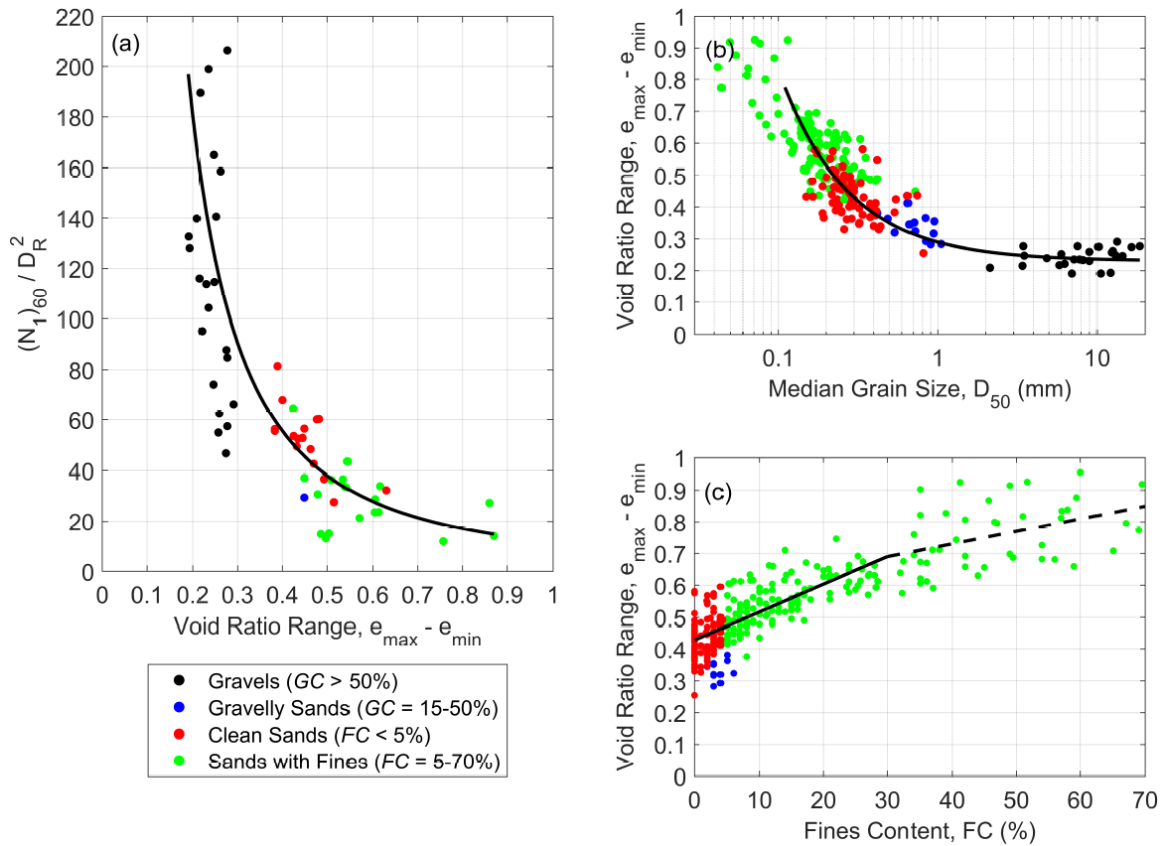


Figure 3. Influence of grain size on void ratio and penetration resistance for sands with fines, clean sands, gravelly sands, and gravels: (a) normalized SPT penetration resistance as a function of void ratio range, (b) void ratio range as a function of median grain diameter, and (c) void ratio range as a function of fines content for sands and silty sands (Cubrinovski and Ishihara, 1999, Cubrinovski and Ishihara, 2002).

## LABORATORY EVALUATION OF INDEX VOID RATIOS

### Framework for the development of a testing method

Conventional laboratory tests for  $e_{max}$  and  $e_{min}$ , such as the one proposed by the Japanese Geotechnical Society [22], herein referred to as the JGS method, have been developed primarily for sands with small amounts of fines (< 10%). Such methods are not applicable to gravelly soils for several reasons. For example, gravel-sized particles are approximately 10 times larger than sands, on average, so one limitation is that the mould size of standard test methods are too small for gravelly soils. While such issues have been considered in the development of test methods such as Japanese Geotechnical Society [23] for the determination of  $e_{max}$  and  $e_{min}$  of gravels, no such standard test is widely adopted, and the applicability of the Japanese Geotechnical Society [23] method to reclaimed G-S-S mixtures have not been studied. This paper presents preliminary results from ongoing efforts at the University of Canterbury (New Zealand) to develop testing procedures for the determining  $e_{max}$  and  $e_{min}$  of gravelly soils, herein referred to as the University of Canterbury Gravel (UCG) method. The UCG procedures are developed by closely following the Japanese Geotechnical Society [23] method.

The framework for the development of the UCG method involves two key phases. The first phase involves calibrating the UCG test method to produce results that are repeatable, which requires a practicable method with well-defined procedures. In this phase, the calibration is performed by varying several variables of the UCG test method for tests on two reference clean sands. Results are compared to  $e_{max}$  and  $e_{min}$  values obtained from the JGS method for sands to provide reference values for comparison. In the second phase, the adopted UCG method is then used to test samples of gravelly soils collected from the CentrePort case study. It is not uncommon for additional issues to be encountered in the second phase, which therefore merits recalibration of the UCG method. In this sense, the two phases described involve an iterative process.

### Overview of the UCG method

Toyoura sand and Albany sand are the two reference clean sands used for the calibration phase, representing fine and coarse sands, respectively. Toyoura sand was imported from Japan, and Albany sand from Australia. In the second series of tests, four

samples of G-S-S mixtures were for determination of  $e_{max}$  and  $e_{min}$  of gravelly soils. These samples include soils collected from borehole drillings [24] and ejected soils on the ground surface collected after liquefaction during the 2016 Kaikōura earthquake [25]. The reclaimed G-S-S fills are well-graded, comprising of approximately 45-75% gravels, 15-40% sands, and 0-15% silts. Key properties of the test material are summarized in Table 1.

Table 1. Soil properties for laboratory index void ratio tests, including size of the test mould used (diameter and height).

Soil	UCG Test Mould Size	$D_{50}$ (mm)	FC
Toyoura	200 mm & 300 mm	0.19	0%
Albany	200 mm & 300 mm	0.41	0%
G-S-S #1	300 mm	4.5	3%
G-S-S #2	300 mm	7.0	2%
G-S-S #3	300 mm	4.0	5%
G-S-S #4	200 mm	3.2	3%

Two key pieces of equipment are required for testing, as shown in Figure 4. The first is a mould of appropriate size for testing of gravelly soil. In developing the UCG method, two cylindrical mould sizes have been considered: 200 mm and 300 mm in height and diameter. Moulds are made of steel and includes a pedestal, welded rods, and three collars (50 mm, 100 mm, and 200 mm in height). Secondly, as the JGS method does not provide enough energy to densify gravelly soil for the determination of  $e_{min}$ , a vibrator was used as in the method of the Japanese Geotechnical Society [23]. The vibrator included an added load and two O-rings to minimize undesirable movement/rotation of the vibrator during the densification process. Other equipment that was used in the development of the UCG method includes a sample mixing tray of adequate size to allow thorough mixing of the dry sample, a stopwatch, digital calipers with an accuracy of 0.01 mm, a carpenter square, a weighing scale with an accuracy of 0.01 kg, and a folding workshop crane capable of lifting at least 50 kg.

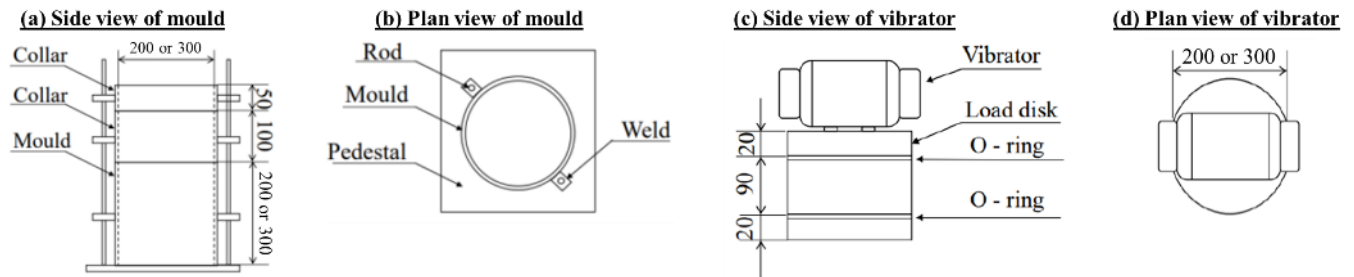


Figure 4. Schematic illustration of the (a & b) mould and (c & d) vibrator used in the UCG test methods (unit of dimensions are mm).

The key steps in the provisional UCG method for  $e_{max}$  are: (i) mix dry sample in a tray and divide it into 10 sub-samples. Each sub-sample should be reasonably representative of the entire sample; (ii) deposit the soil from each sub-sample as loosely as possible by keeping a zero height of deposition, i.e., as close to the surface of the sample as possible; (iii) continue soil deposition until the sample reaches the top collar evenly (with surface height variations of less than 40 mm); (iv) measure soil height using the carpenter square and digital caliper to measure the distance to the top of the soil sample. Measurements are taken at 17 uniformly distributed points and the average height of the soil specimen is estimated. Trial methods have also considered lightly leveling off the surface, or removing the collar and scraping off excess soil, before measuring the soil height. While such approaches work well for sands and silty sand, it is not applicable for gravel-sand-silt mixture including vastly different particle sizes; (v) measure soil weight in the scale to calculate  $e_{max}$ .

The key steps in the provisional UCG method for  $e_{min}$  are: (i) mix dry sample in a tray and divide it into five sub-samples that are deposited into the mould one at a time; (ii) once each layer of soil is placed in the mould, the vibrator is placed on the top of the soil specimen and vibration is applied for 180 seconds, at 38 Hz and 700 N settings of the vibrator; (iii) once the densification by vibration is completed,  $e_{min}$  is estimated by using measured height (volume) and weight of the soil specimen.

### Results from the calibration tests

Summary results using the reference JGS method and the UCG method for the calibration phase of the model development using Toyoura and Albany sands are shown in Table 2. Results indicate generally good repeatability (small range) and consistent  $e_{max}$  and  $e_{min}$  values in the UCG method, though not as repeatable as the JGS method. This is expected as  $e_{max}$  and  $e_{min}$  are a function of the test method and equipment used, which was adjusted slightly in many tests. Generally,  $e_{max}$  was

underestimated and  $e_{min}$  overestimated by the UCG method. Overall, however, the  $e_{max}$  and  $e_{min}$  values are reasonably close to the reference values, suggesting the adopted approach works reasonably well for the reference sands.

Table 2. Laboratory index void ratio calibration tests comparing the Japanese Geotechnical Standard (JGS) and preliminary UCG methods showing number of tests, range of values, and median values.

SOIL Test Type	TOYOURA		ALBANY	
	$e_{max}$	$e_{min}$	$e_{max}$	$e_{min}$
JGS	33 tests Range: 0.89–0.93 Median: 0.92	13 tests Range: 0.59–0.60 Median: 0.60	16 tests Range: 0.81–0.83 Median: 0.83	11 tests Range: 0.53–0.56 Median: 0.55
UCG	6 tests Range: 0.88–0.91 Median: 0.89	7 tests Range: 0.63–0.68 Median: 0.65	11 tests Range: 0.77–0.81 Median: 0.78	7 tests Range: 0.54–0.60 Median: 0.57
Δ Median	0.03	0.05	0.05	0.02

### Results from tests on gravel-sand-silt mixtures

Results of all  $e_{max}$  and  $e_{min}$  tests on the four G-S-S soil specimens are shown in Figure 5. For each specimen, several  $e_{max}$  tests were performed, but only a limited number of the more challenging  $e_{min}$  tests. Three key observations can be made from the results:

- For a given G-S-S sample and test regime, less than 2% variation was observed in the results.
- There is a stark difference in the estimates obtained using the 300 mm mould (G-S-S #1 – #3) and the 200 mm mould (G-S-S #4). This is likely due to particle crushing observed in tests performed in the 300 mm mould, which was not observed in the tests performed using the 200 mm mould. These differences require further investigation.
- The  $(e_{max} - e_{min})$  range is estimated to sit somewhere between that of clean sands and clean gravels (0.3 to 0.4). Therefore, the CI99 relationship for G-S-S mixtures is also expected to be somewhere between the clean sand and clean gravel curves in Figure 2b, illustrating again the usefulness of  $(e_{max} - e_{min})$  as a material parameter to capture the effects of soil grain-size composition on penetration resistance.

It is important to note that the  $e_{max}$  and  $e_{min}$  values for G-S-S mixtures is sensitive to the experimentation details, and therefore, the  $e_{max}$  and  $e_{min}$  values presented in this paper should be considered as preliminary results that yet allow us to approximately evaluate  $D_R$  for the gravelly reclamations, as described in the following section.

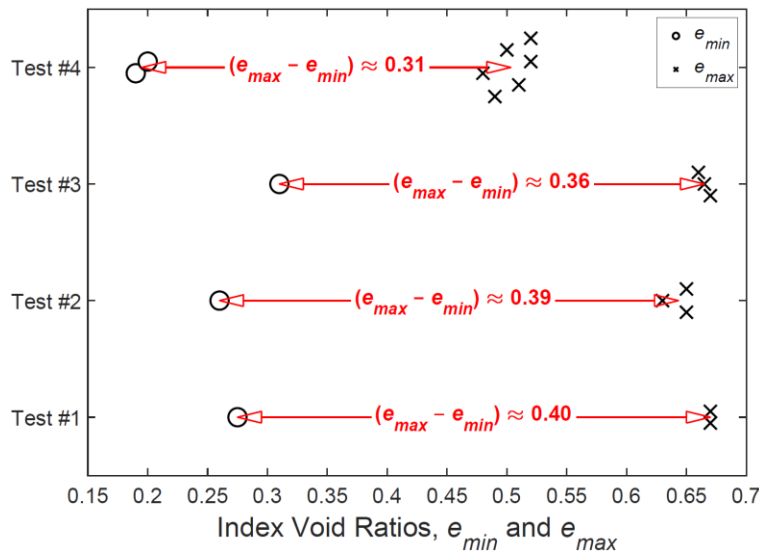


Figure 5. Four sets of preliminary experiments using the UCG method on different G-S-S samples to estimate index void ratios ( $e_{max}$  and  $e_{min}$ ) and void ratio range ( $e_{max} - e_{min}$ ).

### APPLICATION OF RELATIVE DENSITY CORRELATIONS

Using the correlations introduced in Figures 2a and 2b,  $D_R$  is estimated using two CPT profiles shown in Figure 6 and Figure 7, which are then used to calculate post-liquefaction settlement of representative CentrePort fills for the Kaikōura earthquake ( $M_w = 7.8$  and  $PGA = 0.25g$ ). Figure 6 shows a soil profile with continuous G-S-S fill from 3 m to 15 m depth, whereas G-S-S fill from 3 m to 7 m depth overlying a thick layer of sand fill from 7.3 m to 15 m depth is shown in Figure 7. In the figures, the cone tip resistance ( $q_c$ ) and soil behavior type index ( $I_c$ ) profiles are shown alongside  $D_R$  estimates using the three sand-based  $D_R - q_{c1N}$  relationships and the CI99  $D_R - q_{c1N}$  relationship of Eq. (6). Also shown in the figures are calculated  $FS_L$  profiles using both the Robertson & Wride [26] and Boulanger & Idriss [27] methods, and settlement estimates using the Ishihara & Yoshimine [6] method using four different estimates of  $D_R$  from the three sand-based  $D_R - q_{c1N}$ s and G-S-S specific CI99  $D_R - q_{c1N}$  relationships.

Note that the estimates of  $D_R$  using the three sand-based relationships (Eq. (1)–(3)) require a correction of  $q_{c1N}$  to  $q_{c1Ncs}$ , and  $q_{c1N}$  terms in the equation to be replaced with  $q_{c1Ncs}$ . This paper applies the Boulanger & Idriss [27] clean-sand equivalent corrections to IB08, and the Robertson & Wride [26] correction to T90 and RC12, to calculate  $D_R$  and associated settlements. Note that the T90-based settlement estimates are equivalent to the Zhang et al. [2] calculation. The CI99 correlation does not require a correction of  $q_{c1N}$  since different material characteristics are accounted for through ( $e_{max} - e_{min}$ ). Note that the  $D_R$  estimates for CI99 are shown as a shaded range reflecting the adopted range of  $QNR$  and ( $e_{max} - e_{min}$ ) values. The CI99-based settlements are estimated using  $FS_L$  calculated from the BI14  $I_c$ -based method.

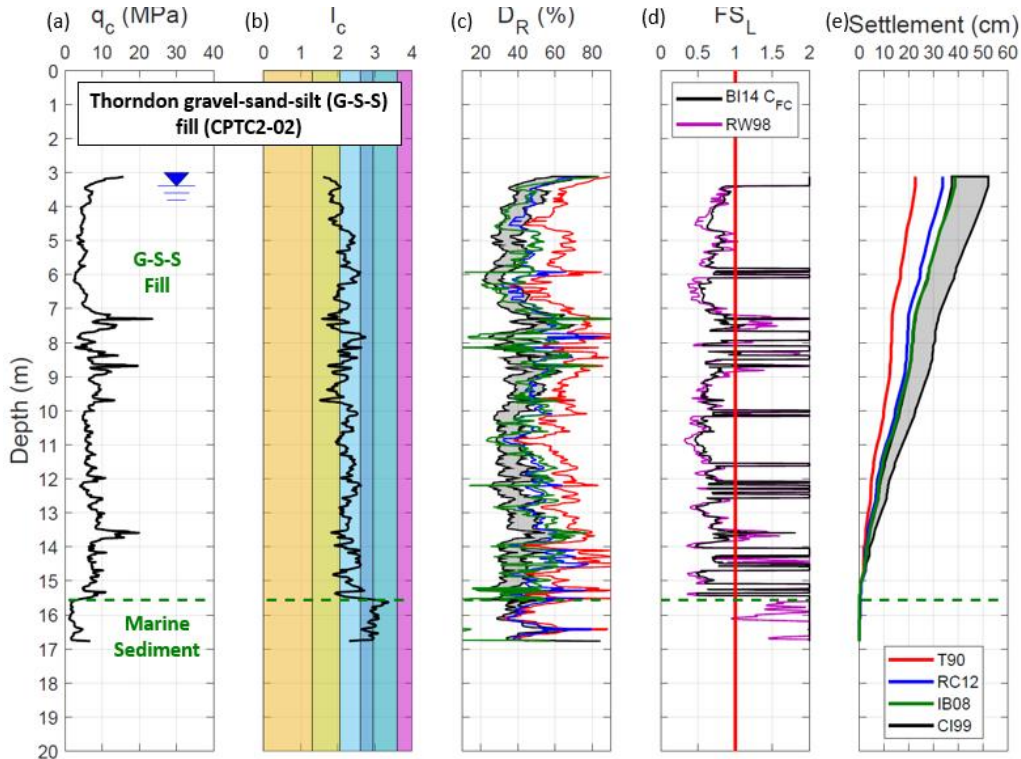


Figure 6. Representative CPT profile containing Thorndon G-S-S fill: (a) cone tip resistance ( $q_c$ ), (b) soil behaviour type index ( $I_c$ ), (c) estimated relative density ( $D_R$ ), (d) factor of safety against liquefaction ( $FS_L$ ), and (e) estimated settlements for the Kaikōura earthquake.



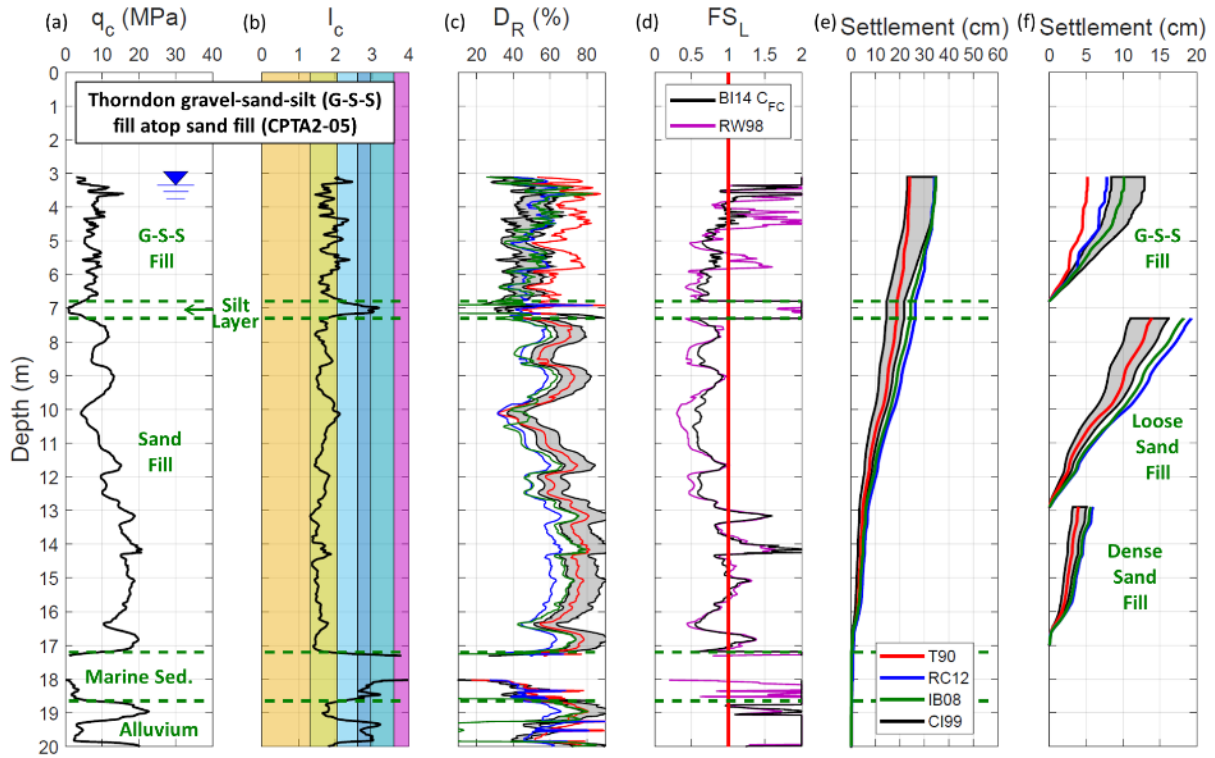


Figure 7. Representative CPT profile containing Thorndon G-S-S fill over thick sand fill: (a) cone tip resistance ( $q_c$ ), (b) soil behaviour type index ( $I_c$ ), (c) estimated relative density ( $D_R$ ), (d) factor of safety against liquefaction ( $FS_L$ ), and estimated settlements for the (e) entire profile and (f) individual soil layers for the Kaikōura earthquake.

The input parameters adopted for the different  $D_R$  relationships are summarized in Table 3 for the three reclamation fills (silt, sand, and G-S-S). A mid-range value of  $C_{dq} = 0.9$  is adopted for the IB08 correlation whereas the value of the coefficient  $c$  in RC12 is assigned based on recommendations by RC12, where  $c$  is smaller for fine-grained soil and increases for coarser material. Empirical evidence shows  $QNR$  increases with median grain size of soils, so  $QNR$  is estimated using typical values for silts and sands based on Robertson et al. [28] and Kulhawy & Mayne [29], and for gravelly soil based on Lunne et al. [30] and Andrus & Youd [31]. Finally,  $(e_{max} - e_{min})$  values for silts and sands are based on the range of typical values from Cubrinovski & Ishihara [5], while  $(e_{max} - e_{min})$  estimates for G-S-S are based on results from the preliminary tests of this paper. The  $D_R$  and settlement estimates for CI99 are shown as a shaded range in Figures 6 and 7 reflecting the adopted range of  $QNR$  and  $(e_{max} - e_{min})$  values. There are significant uncertainties associated with these parameters and empirical relationships that should be acknowledged and accounted for in the engineering interpretation of settlement estimates.

Table 3. Input variables for the IB08, RC12, and CI99 relationships for three soil units identified in Figures 9 and 10.

	$C_{dq}$ (IB08)	$c$ (RC12)	$QNR$ (CI99)	$(e_{max} - e_{min})$ (CI99)
Silt	0.9	300	4	0.65–0.80
Sand	0.9	350	4	0.35–0.45
G-S-S	0.9	400	5–6	0.30–0.40

For the profile dominated by G-S-S fill (Figure 6c), and for the G-S-S part of the fill in Figure 7c (3-7 m depth),  $D_R$  estimates using the IB08 and RC12 correlations are largely 35-60%, which is slightly higher than the CI99 estimated range of  $D_R = 30$ -50%. These values indicate loose to medium-dense G-S-S fill, consistent with the employed construction method of the fill with no compaction effort. The settlement estimates in Figure 6e for the IB08 and RC12 methods (390 mm and 340 mm, respectively) are in the lower end of the CI99 range (370-520 mm). Note, however, that all settlement estimates are based on laboratory established relationships for one clean sand. In contrast, T90 estimates the highest  $D_R = 50$ -70%, which appears somewhat higher than the expected density for the employed construction method and observed liquefaction performance of

the G-S-S fill, and consequently results in the lowest vertical settlement estimate (230 mm). The measured 1D settlement at the location of the CPT in Figure 6 was in the range of 250-400 mm [14].

For the CentrePort G-S-S fill, the sand-based correlations (T90, RC12 and IB08) tend to estimate higher values of  $D_R$  than CI99 for the range of  $(e_{max} - e_{min})$  and  $QNR$  values adopted in Table 3. The proportion of different soil fractions in the G-S-S fill tends to vary [24], hence, G-S-S mixtures with greater fraction of gravels and hence more influence of gravels in the soil matrix will have  $(e_{max} - e_{min})$  values around the adopted lower bound value of 0.3, which is well below the typical  $(e_{max} - e_{min})$  ranges for sands. Consequently, sand-based relationships depict a medium-dense G-S-S deposit as an equivalent dense sand, thus underestimating settlements. For G-S-S mixtures with larger sand and silt content, the upper bound value of  $(e_{max} - e_{min}) = 0.4$  may be more appropriate, which is in the range typical for sand. Hence, in this case, sand-based  $D_R - q_{c1Ncs}$  correlations only slightly overestimate the relative density. The associated settlement underestimation is also relatively small since the overestimated  $D_R$  values remain in the range of loose to medium-dense soil, for which the post-liquefaction volumetric strains are large (Figure 1). Therefore, the conventional CPT-based procedure using sand-based  $D_R - q_{c1Ncs}$  correlations generally provide reasonable settlement estimates for the CentrePort G-S-S fill with a dominant silty sand fraction in the soil matrix, through several compensating mechanisms.

For the soil profile in Figure 7, all four correlations indicate a loose G-S-S fill overlying a looser sand layer (7.3-13 m depth) and a denser sand layer (13-17 m depth). IB08 and RC12 estimate the lowest range of  $D_R$  for the sand layers, with  $D_R = 40-60\%$  and  $60-70\%$  for the shallower and deeper sand layers, respectively (Figure 7c). The CI99 correlation yields  $D_R$  estimates of predominantly 50-70% for the shallower layer and 65-85% for the deeper layer, with the T90 estimates generally within the abovementioned ranges (50-70% and 70-80%, respectively). The estimated settlement for the entire profile using the CI99 relationship is 230-350 mm and all sand-based estimates are within this range. The total measured 1D settlement at the location of the CPT in Figure 7 was 210-250 mm [14].

Because the profile in Figure 7 is not uniform (G-S-S fill overlying loose and dense sand layers), the total estimated settlements in Figure 7e are broken down for each individual soil layer in Figure 7f to depict their separate contributions to the settlement and allow for scrutiny of the employed correlations when applied to different soils. The loose and dense sand layers contribute 110-160 mm and 30-50 mm of the settlement, respectively, in the CI99-based calculation. While the settlement using T90 within the G-S-S fill was the lowest of the four relationships, settlement estimates for both the shallow and deep sand layers are close to the middle of the CI99 range (140 mm and 40 mm, respectively). In contrast, the estimates by IB08 and RC12 are at the higher end of the CI99 range (180-190 mm and 60 mm, respectively). Note, however, that sand-based estimates of settlement in the G-S-S fill are either underestimated (T90) or at the lower end of estimates (IB08 and RC12) as compared to the G-S-S based estimates of CI99. This trend in the G-S-S settlement estimates is consistent with those obtained for the thick and continuous G-S-S fill presented in Figure 6.

Overall,  $D_R$  estimated using the CI99 method can be either below the sand-based estimates for soils with large gravel content exhibiting low  $(e_{max} - e_{min})$ , as shown in Figure 6, or similar to slightly larger than the sand-based estimates for soils exhibiting  $(e_{max} - e_{min})$  values typical of sands, as shown in Figure 7. Compared to the T90, RC12 and IB08 sand-based correlations,  $D_R$  and settlement estimates using CI99 shows the important sensitivity of these estimates to the variation in material characteristics of the fill.

## CONCLUSIONS

In the simplified assessment, liquefaction-induced ground deformations are conventionally estimated using relationships based on laboratory tests on clean sand, which show strong dependence of post-liquefaction volumetric strains ( $\epsilon_v$ ) on the  $D_R$  of the sand. Under the assumption that the  $\epsilon_v - D_R$  relationships derived for clean sand are appropriate for the G-S-S mixtures (which is yet to be confirmed or refuted by experimental evidence), the key issue explored in this paper is the effect of the  $q_{c1Ncs} - D_R$  conversion required for the settlement estimates, specifically for G-S-S fills.  $D_R$  and settlement estimates are made for the CentrePort fills using three  $D_R - q_{c1Ncs}$  relationships developed for sands (T90, RC12 and IB08) and one  $D_R - q_{c1N}$  relationship developed for a wide range of soils including gravelly soils (CI99). Since laboratory tests of index void ratios, which are required for the CI99 correlation, are not standardized in practice for gravelly soil, preliminary results from ongoing efforts to develop an appropriate testing method for evaluation of  $e_{max}$  and  $e_{min}$  for reclaimed G-S-S mixtures is discussed. An approximate value for the void ratio range  $(e_{max} - e_{min}) = 0.3$  to  $0.4$  was obtained for the tested G-S-S soils from CentrePort. The key observations from the subsequent settlement analyses are: (i) Sand-based correlations do not capture the effects of grain-size composition and packing of G-S-S mixtures on their penetration resistance. The CI99 correlation accounts for these effects through the void ratio range  $(e_{max} - e_{min})$  of the soil; (ii) Sand-based correlations tend to estimate either similar or larger values of  $D_R$  for the G-S-S fill, which largely depends on the density state of the fill. Note that estimates of higher  $D_R$  values yield underestimation of settlement as compared to the CI99 estimates. The overestimation of relative density, and hence underestimation of settlement, are smaller for well-graded gravels that have a dominant silty sand fraction in the soil matrix deposited in a loose state; and (iii) Conventional CPT-based procedure in conjunction with sand-based  $D_R - q_{c1Ncs}$  correlations

may significantly underestimate the settlement of medium-dense G-S-S fills and misinterpret those as producing equivalent settlement of a dense sand.

## ACKNOWLEDGMENTS

The authors wish to acknowledge the hard work of the final-year undergraduate project students J.M. Pilet, C.W. Wallis, X. Hong, and C. Mongkolsilpa, who performed all the index void ratio tests in the laboratory and produced Figure 4, and to Dr. S. Rees for his invaluable technical assistance in the University of Canterbury geomechanics laboratory. The presented work is a result of collaborative effort and support from a wide range of organizations and researchers, including contributions from Professor Jonathan Bray (University of California, Berkeley) and the MacMillan Drilling Group who performed the site investigations at CentrePort under the authors' supervision.

## REFERENCES

- [1] Cubrinovski, M. & Dhakal, R. (2021). Identification and Mitigation of Seismic Hazards from Inherited Vulnerabilities, *Proceedings of the 17th World Conference on Earthquake Engineering*, Sendai, Japan.
- [2] Zhang, G., Robertson, P.K. & Brachman, R.W.I. (2002). Estimating liquefaction-induced ground settlements from CPT for level ground, *Canadian Geotechnical Journal*, 39: 1168-1180.
- [3] Cubrinovski, M. (2019). Some important considerations in the engineering assessment of soil liquefaction, *13th Australia New Zealand Conference on Geomechanics*, Perth, Australia.
- [4] Dhakal, R., Cubrinovski, M. & Bray, J.D. (2022). Evaluating the applicability of conventional CPT-based liquefaction assessment procedures to reclaimed gravelly soils, *Soil Dynamics and Earthquake Engineering*, 155: 107176.
- [5] Cubrinovski, M. & Ishihara, K. (1999). Empirical correlation between SPT N-value and relative density for sandy soils, *Soils and Foundations*, 39: 61-71.
- [6] Ishihara, K. & Yoshimine, M. (1992). Evaluation of settlements in sand deposits following liquefaction during earthquakes, *Soils and Foundations*, 32: 173-188.
- [7] Nagase, H. & Ishihara, K. (1988). Liquefaction-induced compaction and settlement of sand during earthquakes, *Soils and Foundations*, 28: 65-76.
- [8] Yoshimine, M., Nishizaki, H., Amano, K. & Hosono, Y. (2006). Flow deformation of liquefied sand under constant shear load and its application to analysis of flow slide of infinite slope, *Soil Dynamics and Earthquake Engineering*, 26: 12.
- [9] Tatsuoka, F., Zhou, S., Sato, T. & Shibuya, S. (1990). Method of evaluating liquefaction potential and its application, Report on Seismic hazards in the soil deposits in urban areas, Ministry of Education of Japan.
- [10] Robertson, P.K. & Cabal, K. (2012). Guide to cone penetration testing, Gregg Drilling & Testing.
- [11] Idriss, I.M. & Boulanger, R.W. (2008). Soil liquefaction during earthquakes, Earthquake engineering research Institute.
- [12] Tokimatsu, K. (1988). Penetration tests for dynamic problems, *International Journal of Rock Mechanics and Mining Sciences and Geomechanics Abstracts*, 27: A90-A90.
- [13] Dhakal, R., Cubrinovski, M., Bray, J.D. & de la Torre, C. (2020). Liquefaction assessment of reclaimed land at CentrePort, Wellington, *Bulletin of the New Zealand Society for Earthquake Engineering*, 53: 12.
- [14] Dhakal, R., Cubrinovski, M. & Bray, J.D. (2020). Geotechnical characterization and liquefaction evaluation of gravelly reclamations and hydraulic fills (Port of Wellington, New Zealand), *Soils and Foundations*, 60: 1507-1531.
- [15] Cubrinovski, M., Bray, J.D., de la Torre, C., Olsen, M.J., Bradley, B.A., Chiaro, G., Stocks, E., Wotherspoon, L. & Krall, T. (2018). Liquefaction-Induced Damage and CPT Characterization of the Reclamations at CentrePort, Wellington, *Bulletin of the Seismological Society of America*, 108: 14.
- [16] Kokusho, T. & Tanaka, Y. (1994). Dynamic properties of gravel layers investigated by in-situ freezing sampling, *Ground Failure under Seismic Condition*, 121-140.
- [17] Evans, M.D. & Zhou, S. (1995). Liquefaction behavior of sand-gravel composites, *Journal of Geotechnical Engineering*, 121: 287-298.
- [18] Cubrinovski, M. & Ishihara, K. (2002). Maximum and minimum void ratio characteristics of sands, *Soils and Foundations*, 42: 65-78.
- [19] Lin, P.S., Chang, C.W. & Chang, W.J. (2004). Characterization of liquefaction resistance in gravelly soil: large hammer penetration test and shear wave velocity approach, *Soil Dynamics and Earthquake Engineering*, 24: 675-687.
- [20] Hara, T., Toyota, H., Takada, S. & Nakamura, K. (2012). Liquefaction characteristic of intermediate soil including gravel, *Proceedings of the 15th World Conference on Earthquake Engineering*, Lisbon, Portugal.
- [21] Dhakal, R. & Cubrinovski, M. (2023). CPT-based evaluation of relative density for reclaimed gravel-sand-silt mixtures, *Proceedings of the 14th Australia and New Zealand Conference on Geomechanics (ANZ2023)*, Cairns, Australia.
- [22] Japanese Geotechnical Society. (2009). Test method for minimum and maximum densities of sands, *JGS 0161-2009*.
- [23] Japanese Geotechnical Society. (2009). Test method for minimum and maximum densities of gravels, *JGS 0162-2009*.

- [24] Dhakal, R. (2022). *Liquefaction Assessment Methodologies for Reclaimed Land; A case study of the port of Wellington, New Zealand (CentrePort)*, PhD Thesis, University of Canterbury, New Zealand.
- [25] Cubrinovski, M., Bray, J., de la Torre, C., Olsen, M., Bradley, B., Chiaro, G., Stock, E. & Wotherspoon, L. (2017). Liquefaction effects and associated damages observed at the Wellington Centreport from the 2016 Kaikōura earthquake, *Bulletin of the New Zealand Society for Earthquake Engineering*, 50: 22.
- [26] Robertson, P.K. & Wride, C.E. (1998). Evaluating cyclic liquefaction potential using the cone penetration test, *Canadian Geotechnical Journal*, 35: 442-459.
- [27] Boulanger, R.W. & Idriss, I.M. (2014). CPT and SPT based liquefaction triggering procedures, Department of Civil & Environmental Engineering, College of Engineering, University of California at Davis.
- [28] Robertson, P.K., Campanella, R. & Wightman, A. (1983). SPT-CPT Correlations, *Journal of Geotechnical Engineering*, 109: 1449-1459.
- [29] Kulhawy, F.H. & Mayne, P.W. (1990). Manual on estimating soil properties for foundation design (No. EPRI-EL-6800), Electric Power Research Inst., Palo Alto, CA (USA); Cornell Univ., Ithaca, NY (USA).
- [30] Lunne, T., Robertson, P.K. & Powell, J. (1997). Cone Penetration Testing in Geotechnical Practice, Abingdon;La Vergne;, Taylor & Francis Group.
- [31] Andrus, R.D. & Youd, T.L. (1987). Subsurface investigation of a liquefaction-induced lateral spread, Thousand Springs Valley, Idaho, *Proceedings of the 22<sup>nd</sup> Symposium on Engineering Geology and Soils Engineering*, Boise, Idaho, USA.